

Hydromagnetic three-dimensional free convection on a vertical stretching surface with heat generation or absorption

Ali J. Chamkha¹

Department of Mechanical and Industrial Engineering, College of Engineering and Petroleum, Kuwait University, P.O. Box 5969, 13060, Safat, Kuwait

Received 2 August 1997; accepted 28 April 1998

Abstract

The problem of steady, laminar, free convection flow over a vertical porous surface in the presence of a magnetic field and heat generation or absorption is considered. The governing three-dimensional partial differential equations for this investigation are transformed into ordinary differential equations using three-dimensional similarity variables. The resulting equations are solved numerically by an accurate, implicit, iterative finite-difference methodology and the obtained results are compared favorably with previously published work. A parametric study is performed to illustrate the influence of the Prandtl number, Hartmann number, heat generation/absorption coefficient, and the surface mass transfer coefficient on the profiles of the velocity components and temperature. Numerical data for the skin-friction coefficient and the Nusselt number functions have been tabulated for various parametric conditions. © 1999 Elsevier Science Inc. All rights reserved.

Keywords: Free convection; Stretching surface; Magnetic field; Heat generation or absorption

1. Introduction

Lately, there has been considerable interest in studying flow and heat transfer characteristics of electrically conducting and heat-generating/absorbing fluids (see for instance, Moalem, 1976; Chakrabarti and Gupta, 1979; Vajravelu and Nayfeh, 1992; Chiam, 1995; Chamkha, 1996; Chandran et al., 1996; Vajravelu and Hadjinalaou, 1997). This interest stems from the fact that hydromagnetic flows and heat transfer have been applied in many industries. For example, in many metallurgical processes such as drawing of continuous filaments through quiescent fluids, and annealing and tinning of copper wires, the properties of the end product depend greatly on the rate of cooling involved in these processes. As mentioned by Vajravelu and Hadjinalaou (1997), the rate of cooling and, therefore, the desired properties of the end product can be controlled by the use of electrically conducting fluids and the application of magnetic fields. The use of magnetic fields has been also used in the process of purification of molten metals from non-metallic inclusions. In addition, due to the significance of the study of flow and heat transfer caused by a stretching surface in many practical manufacturing processes such as extrusion processes, glass blowing, hot rolling, manufacturing of plastic and rubber sheets, crystal growing, continuous coating and fibers spinning, (see Tadmor and Klein, 1970; Fisher, 1976), various aspects of the problem have been considered by many investigators.

Sakiadis (1961a, b) was the first to study boundary-layer flow over a stretched surface moving with a constant velocity. He employed a similarity transformation and obtained a numerical solution for the problem. Later, Erickson et al. (1966) extended the work of Sakiadis (1961a, b) to account for mass transfer at the stretched sheet surface. The numerical results of Sakiadis (1961a, b) were confirmed experimentally by Tsou et al. (1967) and Jacobi (1993) for a continuously moving surface with a constant velocity. Chen and Strobel (1980) and Jacobi (1993) have reported results for uniform motion of the stretched surface. Vajravelu and Hadjinalaou (1997) have considered hydromagnetic convective heat transfer from a stretching surface with a uniform free stream and in the presence of internal heat generation or absorption effects. Many investigations have concentrated on the problem of a stretched sheet with a linear velocity and different thermal boundary conditions (see for instance, Crane, 1970; Vlegaar, 1977; Soundalgekar and Ramana Murty, 1980; Gupta and Gupta, 1977; Carragher and Crane, 1982; Grubka and Bobba, 1985; Dutta and Gupta, 1988; Chen and Char, 1988).

Very recently, many investigations studying the consequent flow and heat transfer characteristics that are brought about by the movement of a stretched permeable and an impermeable, isothermal and nonisothermal surface with a power-law velocity variation have been reported. Examples of these works are Banks (1983) who considered the case of an impermeable wall, Ali (1994–1996) who presented various extensions to Banks (1983) problem in terms of flow and thermal boundary conditions. All of the subsequent references have dealt with two-dimensional flow situations. During the last decade or so, Wang (1984) considered steady three-dimensional flow due to

¹ E-mail: chamkha@kuc01.kuniv.edu.kw

a stretching flat surface. Surma Devi et al. (1986) have studied unsteady three-dimensional boundary-layer flow due to a stretching surface. Lakshmisha et al. (1988) reported numerical solutions for three-dimensional unsteady flow with heat and mass transfer over a continuous stretching surface. Gorla and Sidawi (1994) have reported similarity transformations and numerical solutions for the problem of steady, three-dimensional free convection flow on a stretching surface with suction and blowing.

Motivated by the above investigations and possible applications, it is of interest in the present work to study hydro-magnetic natural convection heat transfer for steady, three-dimensional flow over a linearly stretching sheet with surface mass transfer and heat generation or absorption effects.

2. Problem formulation

Consider steady, laminar, free convection flow of an electrically conducting and heat generating/absorbing fluid over a semi-infinite porous vertical plate stretching in the x -direction with a velocity bx . The y -direction makes an angle α with the horizontal line while the z -direction is normal to the plate surface. A uniform magnetic field is applied in the y -direction which produces magnetic effects in both the x and z directions. This is done in this way so as to allow suppression of convective flow in the these directions. This is important in terms of controlling the quality of the product being stretched (see Vajravelu and Hadjinalaou, 1997). In addition, uniform suction or injection is imposed at the plate surface in the z -direction. The coordinate system and flow model are shown in Fig. 1. All fluid properties are assumed constant except the density in the buoyancy terms of the x - and y -momentum equations. Assuming that the edge effects are negligible, all dependent variables will be independent of the y -direction (Gorla and Sidawi, 1994). In addition, the magnetic Reynolds number is assumed small so that the induced magnetic field is neglected. It is also assumed that all of the Hall effect of magnetohydrodynamics, Joule heating, and the viscous dissipation are negligible and that there is no applied electric field. Under the usual boundary-layer and Boussinesq approximations, the governing equations for this problem can be written as

$$\frac{\partial u}{\partial x} + \frac{\partial w}{\partial z} = 0, \tag{1}$$

$$u \frac{\partial u}{\partial x} + w \frac{\partial u}{\partial z} = \nu \frac{\partial^2 u}{\partial z^2} + g\beta(T - T_\infty) \cos \alpha - \frac{\sigma}{\rho} B_0^2 u, \tag{2}$$

$$w \frac{\partial v}{\partial z} = \nu \frac{\partial^2 v}{\partial z^2} + g\beta(T - T_\infty) \sin \alpha, \tag{3}$$

$$w \frac{\partial w}{\partial z} = -\frac{1}{\rho} \frac{\partial p}{\partial z} + \nu \frac{\partial^2 w}{\partial z^2} - \frac{\sigma B_0^2}{\rho} w, \tag{4}$$

$$w \frac{\partial T}{\partial z} = \frac{\nu}{\text{Pr}} \frac{\partial^2 T}{\partial z^2} + \frac{Q_0}{\rho c_p} (T - T_\infty), \tag{5}$$

where x , y , and z are the coordinate directions. u , v , w , p , and T are the fluid velocity components in the x , y , and z directions, pressure and temperature, respectively. ρ , ν , c_p , and Pr are the fluid density, kinematic viscosity, specific heat at constant pressure, and the Prandtl number, respectively. g , β , T_∞ , and α are the gravitational acceleration, coefficient of thermal expansion, ambient temperature, and the inclination angle, respectively. σ , B_0 , and Q_0 are the fluid electrical conductivity, magnetic induction, and dimensional heat generation/absorption coefficient, respectively. It is a known fact that in a physical application such as crystal growing the heat generation or absorption effect in the fluid is greatly dependent on temperature. Vajravelu and Nayfeh (1992) and Vajravelu and Hadjinalaou (1997) have represented this dependence by a linear relationship. Following these authors, the heat generation or absorption term (last term) of Eq. (5) is assumed to vary linearly with the difference of the fluid temperature in the boundary layer and the ambient temperature.

The boundary conditions suggested by the physics of the problem are:

$$\begin{aligned} u(x, 0) &= bx, & v(x, 0) &= 0, & w(x, 0) &= w_0, \\ T(x, 0) &= T_w, & u(x, \infty) &= 0, & v(x, \infty) &= 0, \\ \frac{\partial w}{\partial z}(x, \infty) &= 0, & T(x, \infty) &= T_\infty \end{aligned} \tag{6}$$

where w_0 and T_w are the wall suction or injection velocity and temperature, respectively.

Following Gorla and Sidawi (1994), it is convenient to use the following similarity transformations:

$$\begin{aligned} \eta &= \sqrt{\frac{b}{\nu}} z, & u &= bx\phi'(\eta) + \Gamma \cos \alpha M(\eta), \\ v &= \Gamma \sin \alpha N(\eta), & w &= -\sqrt{b\nu}\phi, & p &= \rho b\nu G(\eta), \\ H(\eta) &= \frac{T - T_\infty}{T_w - T_\infty}, & \Gamma &= \frac{g\beta(T_w - T_\infty)}{b}. \end{aligned} \tag{7}$$

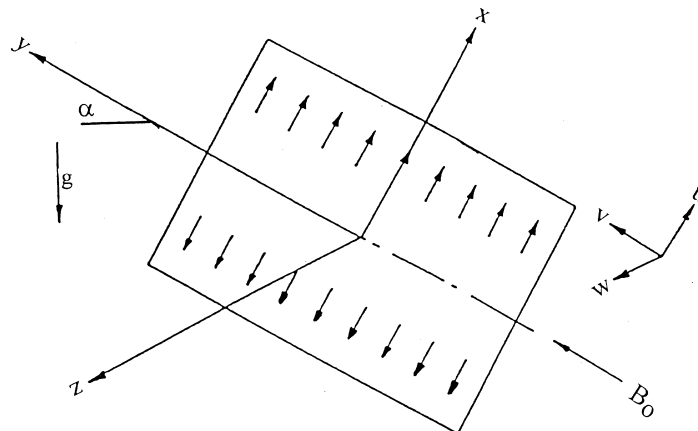


Fig. 1. Problem schematics and coordinate system.

Substituting Eq. (7) into Eqs. (1)–(6) reduces the number of independent variables by one and produces the following similarity equations and boundary conditions:

$$\phi''' + \phi\phi'' - \phi'^2 - \text{Ha}^2\phi' = 0, \quad (8)$$

$$H'' + \text{Pr}\phi H' + \text{Pr}\gamma H = 0, \quad (9)$$

$$N'' + \phi N' + H = 0, \quad (10)$$

$$M'' + \phi M' - M\phi' - \text{Ha}^2 M + H = 0, \quad (11)$$

$$G' + \phi'' + \phi\phi' - \text{Ha}^2\phi = 0, \quad (12)$$

$$\begin{aligned} \phi(0) &= \phi_w, & \phi'(0) &= 1, & \phi'(\infty) &= 0, \\ H(0) &= 1, & H(\infty) &= 0, & N(0) &= 0, & N(\infty) &= 0, \\ M(0) &= 0, & M(\infty) &= 0, & G(0) &= 0, \end{aligned} \quad (13)$$

where a prime denotes ordinary differentiation with respect to η and $\text{Ha}^2 = \sigma B_0^2 / (\rho b)$, $\gamma = Q_0 / (\rho c_p b)$ and $\phi_w = -w_0 / \sqrt{bv}$ are the square of the magnetic Hartmann number, the dimensionless heat generation/absorption coefficient, and the wall mass transfer coefficient, respectively. It should be noted that positive values of ϕ_w indicate fluid suction at the plate surface while negative values of ϕ_w indicate fluid blowing or injection at the wall.

Important physical parameters for this flow and heat transfer situation are the skin-friction coefficients in the x and y directions and the local Nusselt number. The shear stresses at the stretching surface are given by

$$\tau_{zx} = \mu \frac{\partial u}{\partial z}(x, 0) = \rho \sqrt{bv}(bx\phi''(0) + \Gamma \cos \alpha M'(0)), \quad (14)$$

$$\tau_{zy} = \mu \frac{\partial v}{\partial z}(x, 0) = \rho \sqrt{bv}\Gamma \sin \alpha N'(0), \quad (15)$$

where $\mu (= \rho\nu)$ is the dynamic viscosity of the fluid. Upon nondimensionalization of τ_{zx} and τ_{zy} by $\rho(bx)^2/2$, the following respective expressions for the skin-friction coefficients in the x and y directions result:

$$C_{fx} = \frac{2}{\text{Re}_x} \left(\frac{\text{Gr}_x}{\text{Re}_x^2} \cos \alpha M'(0) - 1 \right), \quad (16)$$

$$C_{fy} = \frac{2}{\text{Re}_x \text{Re}_x^2} \sin \alpha N'(0), \quad (17)$$

where $\text{Gr}_x = g\beta(T_w - T_\infty)x^3/\nu^2$ and $\text{Re}_x = bx^2/\nu$ are the local Grashof and Reynolds numbers, respectively.

The local wall heat flux is given by Fourier's law of conduction

$$q_w = -k \frac{\partial T}{\partial z}(x, 0) = -k \sqrt{\frac{b}{v}}(T_w - T_\infty)H'(0), \quad (18)$$

where k is the thermal conductivity of the fluid.

The local Nusselt number can be defined as

$$\text{Nu}_L = \frac{hL}{k} = \frac{q_w L}{k(T_w - T_\infty)} = -\sqrt{\text{Re}_L} H'(0), \quad (19)$$

where h is the local heat transfer coefficient, L is a characteristic plate length, and $\text{Re}_L = bL^2/\nu$ is the Reynolds number at $x = L$.

3. Numerical method

The transformation of the governing partial differential equations into ordinary ones using similarity variables reduced the numerical work significantly. Eqs. (8)–(12) subject to the

boundary conditions (13) are nonlinear and obviously possess no analytical solutions. Therefore, a fully numerical solution of the problem is needed. The implicit, iterative, tri-diagonal finite-difference method discussed by Blottner (1970) and which is similar to the Keller's box method (see Cebeci and Bradshaw, 1977) has proven to be successful for obtaining accurate results for this type of equations. Therefore, it is adopted for the solution of the present problem.

A nonuniform grid distribution in the η direction with a small initial step size was used to accommodate steep changes in the velocity and temperature gradients in the immediate vicinity of the wall. The initial step size employed was $\Delta\eta_1 = 0.001$ and the growth factor was $K = 1.03$ such that $\Delta\eta_{i+1} = K\Delta\eta_i$. The maximum number of grid points used for the parametric study was 195 which gives $\eta_\infty = 10$. The independence of the results from the mesh density was insured and successfully checked by various trial and error numerical experiments.

Eq. (8) was converted into a second-order ordinary differential equation by letting $F = \phi'$. Then, the resulting equation in F along with Eqs. (9)–(11) were discretized using three-point central difference quotients while the equation $\phi' - F = 0$ and Eq. (12) were discretized by the trapezoidal rule. Linear tri-diagonal algebraic equations resulted which were solved by the Thomas algorithm (see Blottner, 1970) with iteration being employed to deal with the nonlinearities of the governing equations. A convergence criterion based on the relative difference between the current and the previous iterations was utilized. When this difference reached 10^{-5} , the solution was assumed converged and the iteration procedure was terminated. A representative set of graphical results for water ($\text{Pr} = 6.7$) flow along an impermeable surface ($\phi_w = 0$) with slight heat absorption effect ($\gamma = -0.1$) and in the presence of a magnetic field ($\text{Ha} = 1$) as a reference is presented in Figs. 2–19 to illustrate the physical influence of the magnetic Hartmann number Ha , the wall mass transfer coefficient ϕ_w , the Prandtl number Pr , and the dimensionless heat generation/absorption coefficient γ on the solutions. The reference parametric values used may or may not represent a physical situation but they are used for the sake of carrying out the parametric study.

4. Results and discussion

Figs. 2–7 present typical profiles for the variables of the fluid's x -component of velocity (ϕ' and M), y -component of velocity (N), z -component of velocity (ϕ), pressure (G), and the temperature (H) for various values of the magnetic Hartmann number Ha , respectively. Application of a magnetic field in the y -direction has a tendency to produce resistive forces in both the x and z directions and to induce higher flow rates in the y -direction. This has the effects of reducing the x and z components of velocity and increasing the y -component of velocity. These behaviours are evident by the decreases in ϕ' , M , and ϕ and the increases in N shown in Figs. 2–5, respectively. In addition, as is clear from Eq. (12), the fluid's pressure G increases as Ha increases so as to overcome the last term of Eq. (12) and maintain the balance of the terms appearing in the equation. Similarly, the decreases in the values of ϕ as Ha increases lead to increases in the fluid's temperature H to overcome the decreases in the convective term of Eq. (9) and maintain the equality of the equation. Both of these facts are illustrated in Figs. 6 and 7, respectively.

Figs. 8–13 show the influence of the mass transfer coefficient ϕ_w on the flow and thermal profiles ϕ' , M , N , ϕ , G , and H , respectively. It is a known fact that imposition of fluid suction ($\phi_w > 0$) at a surface reduces the region of viscous domination close to the wall. For the present problem, this has the ten-

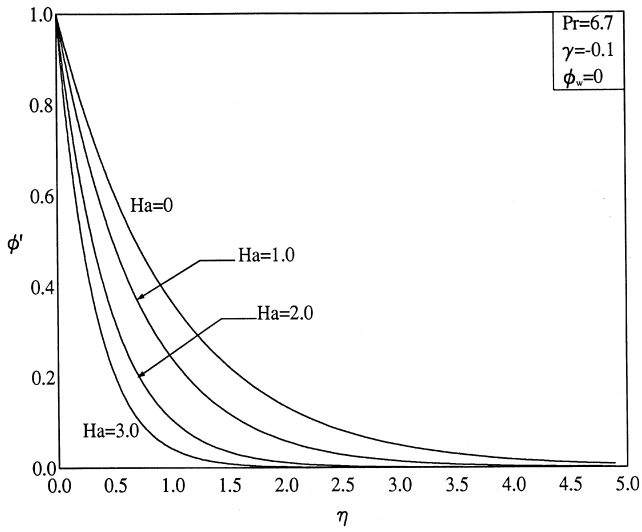


Fig. 2. Effects of Ha on ϕ' (x -component of velocity) profiles.

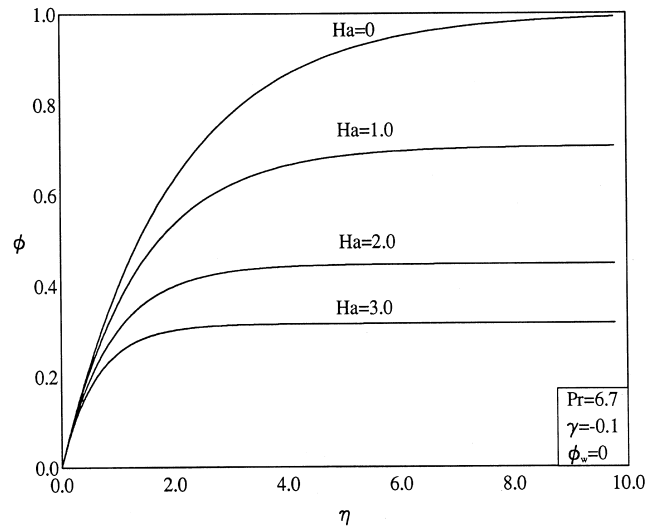


Fig. 5. Effects of Ha on z -component of velocity profiles.

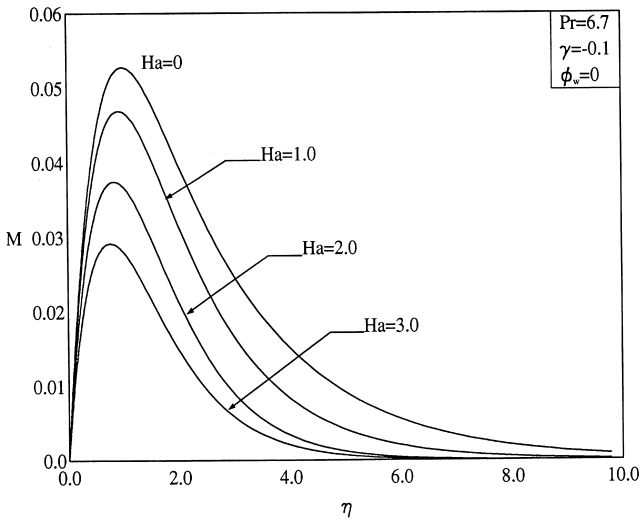


Fig. 3. Effects of Ha on M (x -component of velocity) profiles.

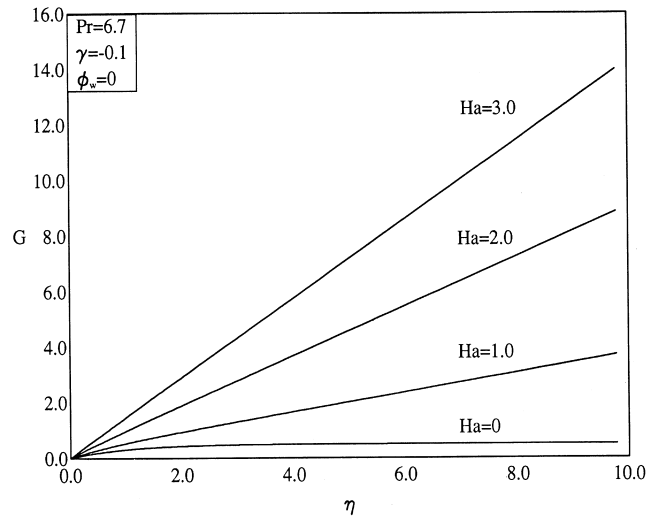


Fig. 6. Effects of Ha on pressure-profiles.

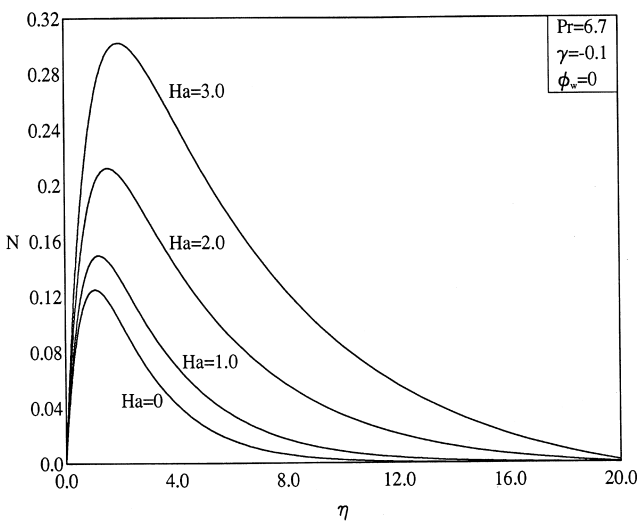


Fig. 4. Effects of Ha on y -component of velocity profiles.

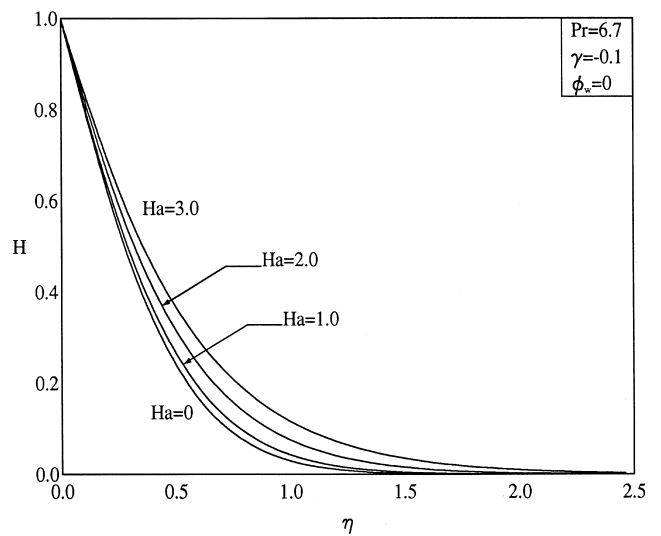


Fig. 7. Effects of Ha on temperature profiles.

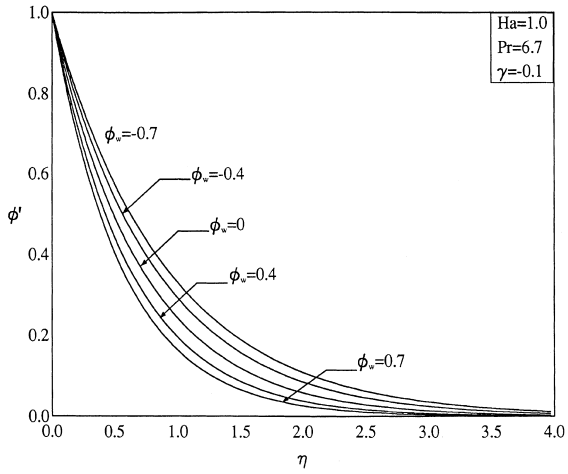


Fig. 8. Effects of ϕ_w on ϕ' (x -component of velocity) profiles.

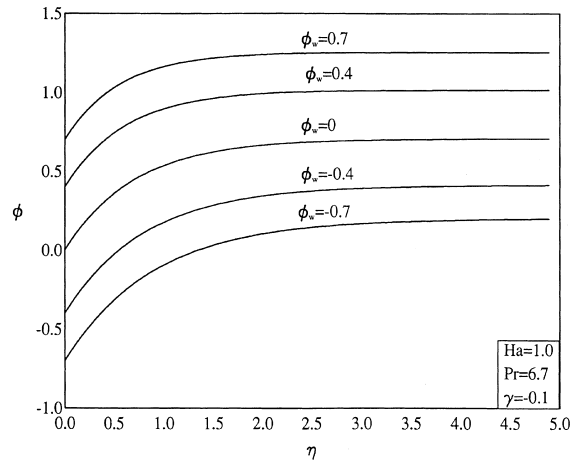


Fig. 11. Effects of ϕ_w on z -component of velocity profiles.

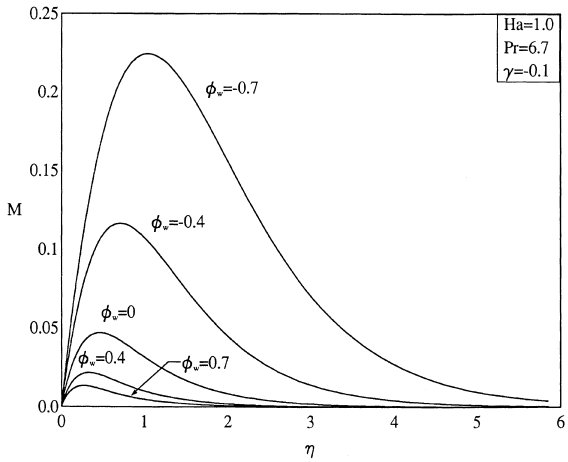


Fig. 9. Effects of ϕ_w on M (x -component of velocity) profiles.

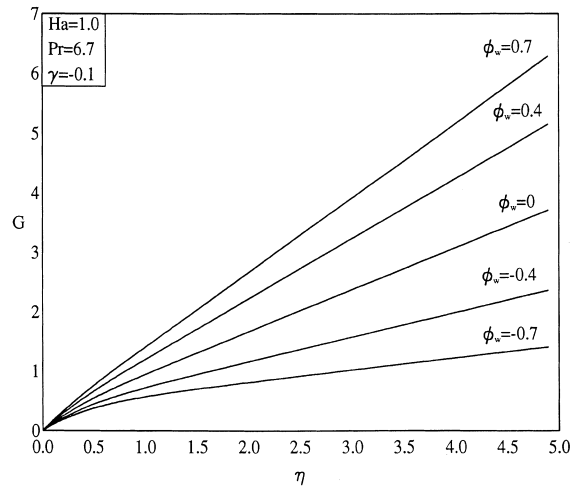


Fig. 12. Effects of ϕ_w on pressure profiles.

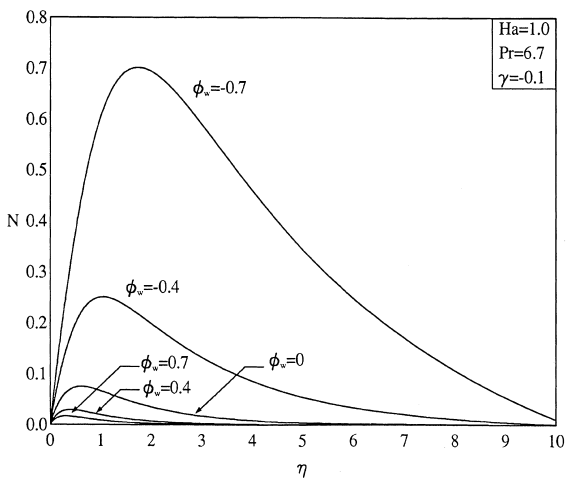


Fig. 10. Effects of ϕ_w on γ -component of velocity profiles.

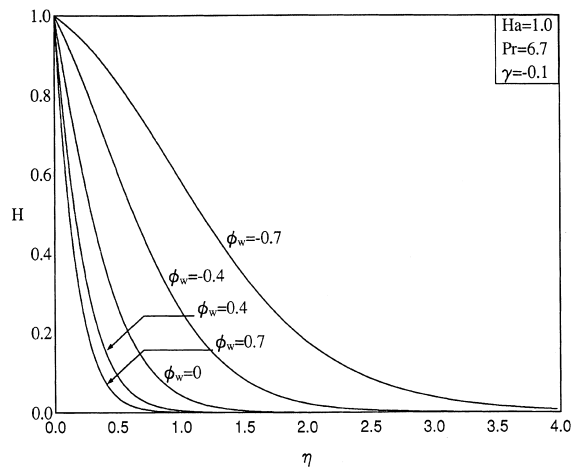


Fig. 13. Effects of ϕ_w on temperature profiles.

dency to reduce the fluid’s velocity components in the x and y directions and increase its velocity component in the z -direction. On the other hand, blowing or injecting fluid ($\phi_w < 0$) from the porous surface into the main stream of the flow produces the opposite effect, that is, increases in the x and y velocity components and decreases in the velocity component in the z -direction. It should be noted that $\phi(\eta)$ approaches a constant value at η_∞ and the values of $\phi(\infty)$ represent a measure of the entrainment velocity. Thus, higher entrainment velocities are produced with higher wall suction velocities. These behaviours are clearly depicted in the decreases in all of the variables ϕ' , M , and N , and the increases in the variable ϕ as the wall mass transfer coefficient ϕ_w increases shown in Figs. 8–11, respectively. In addition, increases in the values of ϕ_w cause increases in the fluid’s pressure distribution G and decreases in the thermal layer close to the wall and the fluid’s temperature distribution H . These facts are given in Figs. 12 and 13, respectively.

The effects of the Prandtl number Pr on the flow and thermal profiles M , N , and H are presented in Figs. 14–16, respectively. It is obvious that Eqs. (8) and (12) are uncoupled from the other equations. Therefore, changes in the values of Pr will cause no changes in the profiles of ϕ' , ϕ , and G . For this reason, no figures for these variables are presented herein. As the Prandtl number Pr increases, both the fluid hydrodynamic and thermal boundary layers decrease. Thus, all the fluid’s velocity components (except the z -component) as well as its temperature decrease at every point above the plate. This is evident from the decreases in M , N and H as Pr increases as reported in Figs. 14–16, respectively.

Figs. 17–19 depict the respective changes in the profiles of M , N , and H as the dimensionless heat generation/absorption coefficient γ is changed. No figures for ϕ' , ϕ , and G are presented herein for the same reason as mentioned in the previous paragraph. In contrast with Pr , it is clear from Figs. 17–19 that increasing the values of γ produces increases in the velocity and temperature distributions of the fluid. This is expected since heat generation ($\gamma > 0$) causes the thermal boundary layer to become thicker and the fluid to become warmer. This enhances the effect of the thermal buoyancy of the driving body force due to mass density variations which are coupled to the temperature distribution and, therefore, increasing the fluid velocity distribution. On the contrary, heat absorption ($\gamma < 0$) has the opposite effect, namely cooling of the fluid, reducing the thermal buoyancy effect, and reducing the fluid velocity field.

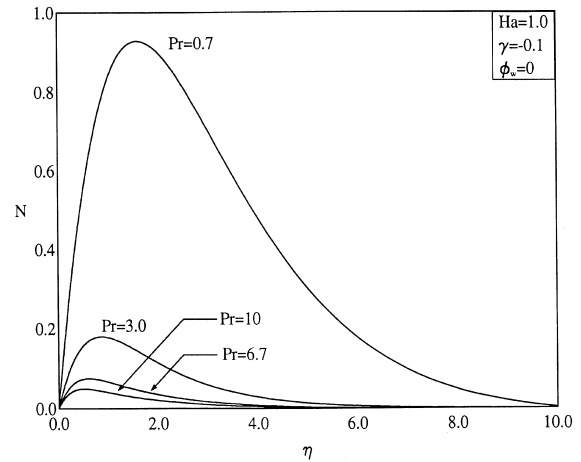


Fig. 15. Effects of Pr on y -component of velocity profiles.

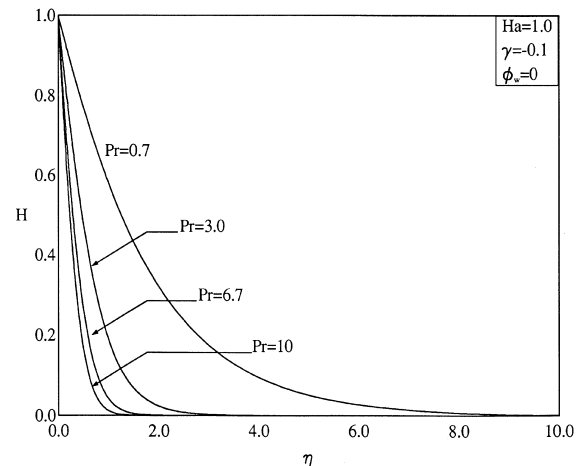


Fig. 16. Effects of Pr on temperature profiles.

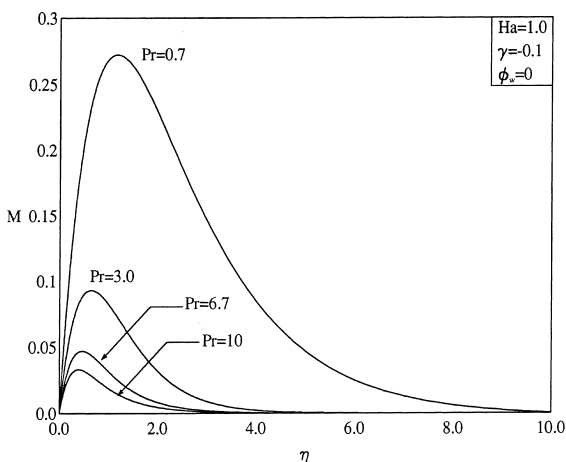


Fig. 14. Effects of Pr on M (x -component of velocity) profiles.

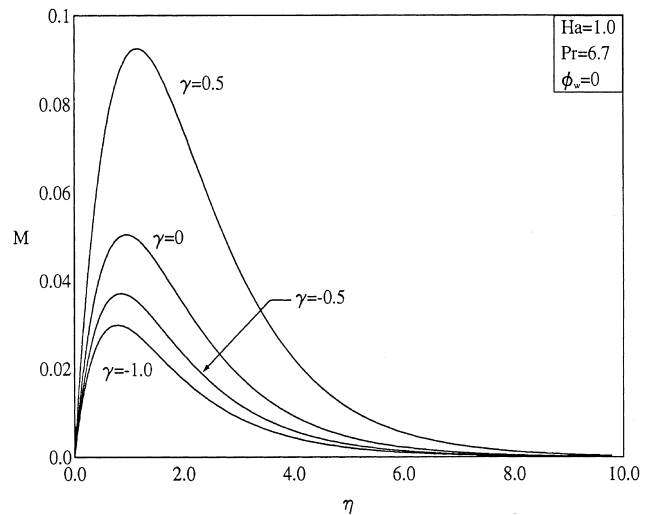


Fig. 17. Effects of γ on M (x -component of velocity) profiles.

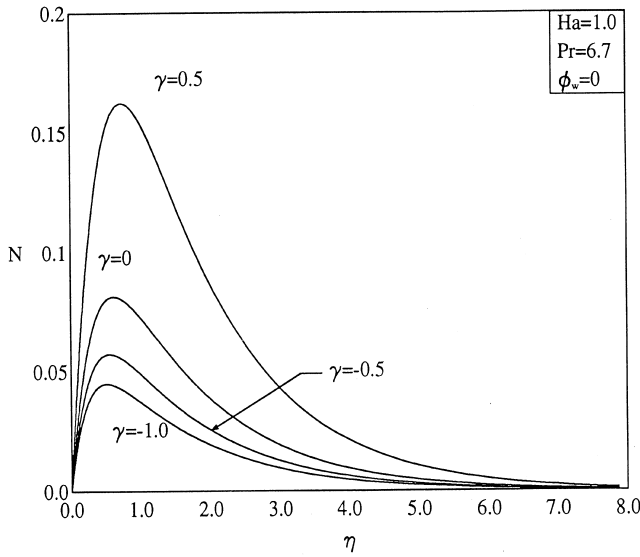


Fig. 18. Effects of γ on y -component of velocity profiles.

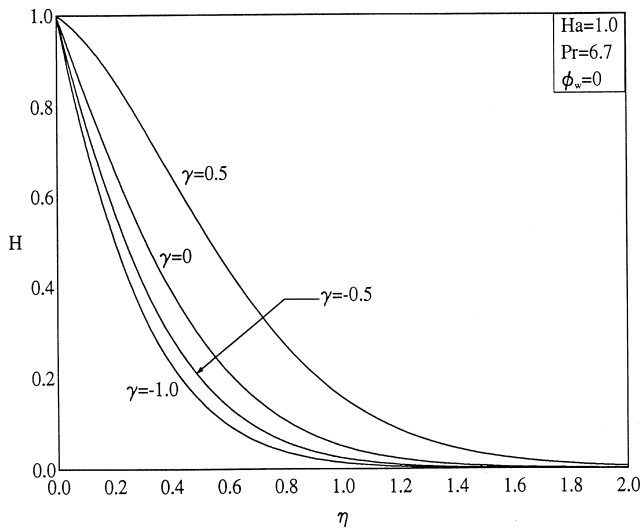


Fig. 19. Effects of γ on temperature profiles.

Table 1 shows a comparison of the present results for $\phi''(0), H'(0), N'(0),$ and $M'(0)$ with those reported by Gorla and Sidawi (1994) for various Pr and ϕ_w values in the absence of magnetic ($Ha = 0$) and heat generation/absorption ($\gamma = 0$) effects. It can be seen from this table that the comparison is excellent for higher values of Pr and smaller values of ϕ_w , while it is not so for smaller values of Pr and higher values of ϕ_w . There appear to be some errors associated with the results of Gorla and Sidawi (1994). This is probably related to their numerical scheme employed to solve two-point boundary-value problems. It is a known fact that there can be serious difficulties with this numerical scheme. Among these are instability (see Nakamura, 1991), convergence difficulties from poor starting approximations, and difficulties related to infinite endpoints as is the case in the present problem. These difficulties are also discussed by the authors (Gorla and Sidawi, 1994). Comparison of Fig. 9 in the present work and Fig. 5 in

Table 1
Comparison of $\phi''(0), H'(0), N'(0)$ and $M'(0)$ with those of Gorla and Sidawi (1994) for various Pr and ϕ_w values and $Ha = 0$ and $\gamma = 0$

Pr	ϕ_w	$\phi''(0)$, Present work	$\phi''(0)$, Gorla and Sidawi (1994)	$H'(0)$, Present work	$H'(0)$ Gorla and Sidawi (1994)	$N'(0)$, Present work	$N'(0)$, Gorla and Sidawi (1994)	$M'(0)$, Present work	$M'(0)$, Gorla and Sidawi (1994)
0.7	0	-1.00180	-1.01435	-0.45593	-0.53488	1.20055	0.81521	0.94332	0.69620
3.0	0	-1.00180	-1.01435	-1.16669	-1.15970	0.48829	0.47431	0.42834	0.42337
7.0	0	-1.00180	-1.01435	-1.89691	-1.89046	0.30906	0.30554	0.28267	0.28197
2.0	0	-1.00180	-1.01435	-3.35574	-3.35391	0.17984	0.17964	0.17026	0.17045
70.0	0	-1.00180	-1.01435	-6.46576	-6.46221	0.09552	0.09562	0.09268	0.09271
7.0	-0.7	-0.71130	-0.72252	-0.09320	-0.08715	0.73108	0.69711	0.59230	0.58929
7.0	-0.4	-0.82166	-0.83420	-0.50906	-0.50012	0.52034	0.50709	0.44822	0.44702
7.0	0.4	-1.22141	-1.23180	-3.99445	-3.98932	0.19578	0.19490	0.18551	0.18525
7.0	0.7	-1.41107	-1.41884	-5.80475	-5.30002	0.14805	0.03024	0.14254	0.02741

Table 2

Values of $\phi''(0)$, $H'(0)$, $N'(0)$ and $M'(0)$ for various values of ϕ_w and $\text{Pr}=6.7$, $\text{Ha}=1.0$ and $\gamma=-0.1$

ϕ_w	$\phi''(0)$	$-H'(0)$	$N'(0)$	$M'(0)$
-0.7	-1.10843	0.22659	0.88223	0.49759
-0.4	-1.23001	0.62473	0.58555	0.39671
0.0	-1.41602	1.93707	0.32932	0.26234
0.4	-1.62943	3.92636	0.20487	0.17816
0.7	-1.80872	5.64584	0.15430	0.13946

Table 3

Values of $\phi''(0)$, $H'(0)$, $N'(0)$ and $M'(0)$ for various values of Pr and $\text{Ha}=1.0$, $\gamma=-0.1$ and $\phi_w=0$

Pr	$\phi''(0)$	$-H'(0)$	$N'(0)$	$M'(0)$
0.7	-1.41602	0.48416	1.36112	0.61911
3.0	-1.41602	1.21240	0.52705	0.36982
6.7	-1.41602	1.93707	0.32932	0.26234
10	-1.41602	2.42590	0.26363	0.21948
100	-1.41602	8.25092	0.07885	0.07453

Table 4

Values of $\phi''(0)$, $H'(0)$, $N'(0)$ and $M'(0)$ for various values of Ha and $\text{Pr}=6.7$, $\gamma=-0.1$ and $\phi_w=0$

Ha	$\phi''(0)$	$-H'(0)$	$N'(0)$	$M'(0)$
0	-1.00180	2.01520	0.30358	0.27781
1	-1.41602	1.93707	0.32932	0.26234
2	-2.23731	1.79053	0.38625	0.23241
3	-3.16351	1.64569	0.45423	0.20175
5	-5.10068	1.42032	0.58323	0.15257

Table 5

Values of $\phi''(0)$, $H'(0)$, $N'(0)$ and $M'(0)$ for various values of γ and $\text{Pr}=6.7$, $\text{Ha}=1.0$ and $\phi_w=0$

γ	$\phi''(0)$	$-H'(0)$	$N'(0)$	$M'(0)$
-1.0	-1.41602	3.12466	0.24481	0.20418
-0.5	-1.41602	2.53280	0.28152	0.22996
0	-1.41602	1.76056	0.34627	0.27355
0.5	-1.41602	0.40872	0.53057	0.38888

the paper by Gorla and Sidawi (1994) shows clearly that at $\eta=3$, the value of $M(\eta)$ is far from zero even in the presence of magnetic and heat absorption effects. This confirms that the infinite end point is not approximated adequately by the previous authors. It should be mentioned here that, in the present work, separate runs were also made by the Runge–Kutta Method which proved the correctness of the numerical results presented in this paper.

Table 2 displays the effects of ϕ_w on the wall values of ϕ'' , H' , N' , and M' for finite values of Ha and γ . It is seen that imposition of suction increases the wall heat transfer rate ($-H'(0)$) and decreases the skin-friction coefficients in the x and y directions.

Table 3 presents values for ϕ'' , H' , N' , and M' at the wall for various values of Pr for an impermeable wall. It is clearly seen from this table that similar to ϕ_w , increases in the values of Pr increase the wall heat transfer and decrease the wall shear stresses in both the x and y directions while it has no influence on $\phi''(0)$.

Table 4 illustrates the effects of increasing the strength of the magnetic field (Ha) on the parameters presented in the previous tables. It can be observed that as Ha increases, both

the local Nusselt number ($-H'(0)$) and the skin-friction coefficient in the x -direction ($M'(0)$) decrease while the skin-friction coefficient in the y -direction ($N'(0)$) increases.

Finally, the effects of the heat generation/absorption coefficient γ on the values of $\phi''(0)$, $H'(0)$, $N'(0)$, and $M'(0)$ are reported in Table 5. As expected and discussed before, γ has no effect on ϕ and, therefore, it has no effect on $\phi'(0)$. However, as γ increases the wall heat transfer decreases while the skin-friction coefficients increase.

5. Conclusion

The problem of steady, laminar free convection from a vertical stretching surface in the presence of magnetic, heat generation/absorption, and wall suction/injection effects is investigated numerically by an accurate implicit finite-difference method. Numerical results for the velocity and temperature profiles are presented graphically for various parametric conditions. In addition, the slopes for the velocity and thermal functions are tabulated for different values of the wall mass transfer coefficient, Prandtl number, Hartmann number, and

the dimensionless heat generation/absorption coefficient. It was found that imposition of fluid wall suction increased the wall heat transfer and decreased the skin-friction coefficients in both the x and y directions. The same was observed as the fluid Prandtl number was increased. The opposite result was obtained as the dimensionless heat generation coefficient was increased. However, the effects of the magnetic Hartmann number were found to be decreasing the wall heat transfer and the skin-friction coefficients in the x direction while increasing the skin-friction coefficient in the y direction. It is hoped that the similarity results presented in the present work will serve as a benchmark for other related studies and be useful for design and analysis of systems involving similar flow and heat transfer situations.

References

- Ali, M.E., 1994. Heat transfer characteristics of a continuous stretching surface. *Wärme-rund Stoffübertragung* 29, 227–234.
- Ali, M.E., 1995. On thermal boundary layer on a power-law stretched surface with suction or injection. *Int. J. Heat and Fluid Flow* 16, 280–290.
- Ali, M.E., 1996. The effect of suction or injection on the laminar boundary layer development over a stretched surface, *J. King Saud Univ., Eng. Sci.* 1, p. 8 (in press).
- Banks, W.H.H., 1983. Similarity solutions of the boundary-layer equations for a stretching wall. *J. Mécanique Théorique et Appliquée* 2, 375–392.
- Blottner, F.G., 1970. Finite-difference methods of solution of the boundary-layer equations. *AIAA J.* 8, 193–205.
- Carragher, P., Crane, L.J., 1982. Heat transfer on a continuous stretching sheet. *ZAMM* 62, 564–565.
- Cebeci, T., Bradshaw, P., 1977. *Momentum Transfer in Boundary Layers*. Hemisphere, Washington, DC.
- Chakrabarti, A., Gupta, A.S., 1979. Hydromagnetic flow and heat transfer over a stretching sheet. *Q. Appl. Math.* 37, 73–78.
- Chamkha, A.J., 1996. Non-darcy hydromagnetic free convection from a cone and a wedge in porous media. *Int. Commun. Heat Mass Transfer* 23, 875–887.
- Chandran, P., Sacheti, N.C., Singh, A.K., 1996. Hydromagnetic flow and heat transfer past a continuously moving porous boundary. *Int. Commun. Heat Mass Transfer* 23, 889–898.
- Chen, C.K., Char, M., 1988. Heat transfer of a continuous stretching surface with suction or blowing. *J. Math. Anal. Appl.* 135, 568–580.
- Chen, T.S., Strobel, F.A., 1980. Buoyancy effects in boundary layer adjacent to a continuous moving horizontal flat plate. *J. Heat Transfer* 102, 170–172.
- Chiam, T.C., 1995. Hydromagnetic flow over a surface stretching with a power-law velocity. *Int. J. Engng. Sci.* 33, 429–435.
- Crane, L.J., 1970. Flow past a stretching plane. *Z. Amgew. Math. Phys.* 21, 645–647.
- Dutta, B.K., Gupta, A.S., 1988. Cooling of a stretching sheet in a viscous flow with suction or blowing. *ZAMM* 68, 231–236.
- Erickson, L.E., Fan, L.T., Fox, V.G., 1966. Heat and mass transfer on a moving continuous flat plate with suction or injection. *Indust. Eng. Chem.* 5, 19–25.
- Fisher, E.G., 1976. *Extrusion of Plastics*. Wiley, New York.
- Gorla, R.S.R., Sidawi, I., 1994. Free convection on a vertical stretching surface with suction and blowing. *Appl. Sci. Res.* 52, 247–257.
- Grubka, L.G., Bobba, K.M., 1985. Heat transfer characteristics of a continuous stretching surface with variable temperature. *J. Heat Transfer* 107, 248–250.
- Gupta, P.S., Gupta, A.S., 1977. Heat and mass transfer on a stretching sheet with suction or blowing. *Can. J. Chem. Engrg.* 55 (6), 744–746.
- Jacobi, A.M., 1993. A scale analysis approach to the correlation of continuous moving sheet, backward boundary layer forced convective heat transfer. *J. Heat Transfer* 115, 1058–1061.
- Lakshmisha, K.N., Venkateswaran, S., Nath, G., 1988. Three dimensional unsteady flow with heat and mass transfer over a continuous stretching surface. *J. Heat Transfer* 110, 590–595.
- Moalem, D., 1976. Steady state heat transfer within porous medium with temperature dependent heat generation. *Int. J. Heat Mass Transfer* 19, 529–537.
- Nakamura, S., 1991. *Applied Numerical Methods with Software*. Prentice-Hall, Englewood Cliffs, NJ.
- Sakiadis, B.C., 1961a. Boundary-layer behavior on continuous solid surfaces: I. boundary-layer equations for two-dimensional and axisymmetric flow. *AIChE J.* 7 (1), 26–28.
- Sakiadis, B.C., 1961b. Boundary-layer behavior on continuous solid surface: II. boundary-layer on a continuous flat surface. *AIChE J.* 7 (1), 221–225.
- Soundalgekar, V.M., Ramana Murty, T.V., 1980. Heat transfer past a continuous moving plate with variable temperature. *Wärme-rund-Stoffübertragung* 14, 91–93.
- Surma Devi, C.D., Takhar, H.S., Nath, G., 1986. Unsteady three-dimensional boundary layer flow due to a stretching surface. *Int. J. Heat and Mass Transfer* 29, 1996–1999.
- Tadmor, Z., Klein, I., 1970. *Engineering principles of plasticating extrusion*. Polymer Science and Engineering Series, Van Nostrand Reinhold, New York.
- Tsou, F.K., Sparrow, E.M., Goldstein, R.J., 1967. Flow and heat transfer in the boundary layer on a continuous moving surface. *Int. J. Heat and Mass Transfer* 10, 219–235.
- Vajravelu, K., Hadjinicalaou, A., 1997. Convective heat transfer in an electrically conducting fluid at a stretching surface with uniform free stream. *Int. J. Engng. Sci.* 35, 1237–1244.
- Vajravelu, K., Nayfeh, J., 1992. Hydromagnetic convection at a cone and a wedge. *Int. Commun. Heat Mass Transfer* 19, 701–710.
- Vleggaar, J., 1977. Laminar boundary-layer behavior on continuous accelerating surfaces. *Chem. Engrg. Sci.* 32, 1517–1525.
- Wang, C.Y., 1984. The three-dimensional flow due to a stretching flat surface. *Phys. Fluids* 27, 1915–1917.